

# Surface location of sodium atoms attached to $^3\text{He}$ nanodroplets

F. Stienkemeier,<sup>1</sup> O. Bünermann,<sup>1</sup> R. Mayol,<sup>2</sup> F. Ancilotto,<sup>3</sup> M. Barranco,<sup>2</sup> and M. Pi<sup>2</sup>

<sup>1</sup>*Fakultät für Physik, Universität Bielefeld, D-33615 Bielefeld, Germany*

<sup>2</sup>*Departament E.C.M., Facultat de Física, Universitat de Barcelona, E-08028, Spain*

<sup>3</sup>*INFM (Udr Padova and DEMOCRITOS National Simulation Center,  
Trieste, Italy) and Dipartimento di Fisica “G. Galilei”,  
Università di Padova, via Marzolo 8, I-35131 Padova, Italy*

(Dated: January 30, 2018)

We have experimentally studied the electronic  $3p \leftarrow 3s$  excitation of Na atoms attached to  $^3\text{He}$  droplets by means of laser-induced fluorescence as well as beam depletion spectroscopy. From the similarities of the spectra (width/shift of absorption lines) with these of Na on  $^4\text{He}$  droplets, we conclude that sodium atoms reside in a “dimple” on the droplet surface and that superfluid-related effects are negligible. The experimental results are supported by Density Functional calculations at zero temperature, which confirm the surface location of sodium on  $^3\text{He}$  droplets, and provide a detailed description of the “dimple” structure. The calculated shift of the excitation spectra for the two isotopes is in good agreement with the experimental data.

PACS numbers: 68.10.-m , 68.45.-v , 68.45.Gd

Detection of laser-induced fluorescence (LIF) and beam depletion (BD) signals upon laser excitation provides a sensitive spectroscopic technique to investigate electronic transitions of chromophores attached to  $^4\text{He}$  nanodroplets [1]. While most of atomic and molecular dopants migrate to the center of the droplet, alkali atoms (and alkaline earth atoms to some extent [2]) have been found to reside on the surface of  $^4\text{He}$  droplets, as evidenced by the much narrower and less shifted spectra when compared to those found in bulk liquid  $^4\text{He}$  [3, 4, 5, 6]. This result has been confirmed by Density Functional (DF) [7] and Path Integral Monte Carlo (PIMC) [8] calculations, which predict surface binding energies of a few Kelvin, in agreement with the measurements of detachment energy thresholds using the free atomic emissions [9]. The surface of liquid  $^4\text{He}$  is only slightly perturbed by the presence of the impurity, which produces a “dimple” on the underlying liquid. The study of these states can thus provide useful information on surface properties of He nanodroplets complementary to that supplied by molecular-beam scattering experiments [10, 11].

Although the largest amount of work has been devoted to the study of pure and doped  $^4\text{He}$  nanodroplets -see [12, 13] and Refs. therein-, the only neutral Fermi systems capable of being observed as bulk liquid and droplets are made of  $^3\text{He}$  atoms, and for this reason they have also attracted the interest of experimentalists and theoreticians [11, 14, 15, 16, 17, 18, 19, 20]. We recall that while  $^4\text{He}$  droplets, which are detected at an experimental temperature ( $T$ ) of  $\sim 0.38$  K, are superfluid, these containing only  $^3\text{He}$  atoms, even though detected at a lower  $T$  of  $\sim 0.15$  K, do not exhibit superfluidity [21].

The behavior of molecules in He clusters is especially appealing. In particular, probes at the surface of the droplets are desirable because they allow to investigate the liquid–vacuum interface as well as droplet surface excitations. The latter are of interest in the compari-

son of the superfluid vs. normal fluid behavior, particularly because the Bose–Einstein condensate fraction has been calculated to approach 100% on the surface of  $^4\text{He}$  [22]. Small  $^3\text{He}$  drops are difficult to detect since, as a consequence of the large zero-point motion, a minimum number of atoms is needed to produce a selfbound drop [15, 16, 17]. Microscopic calculations of  $^3\text{He}$  droplets are scarce, and only concern the ground state (GS) structure [15, 20]. GS properties and collective excitations of  $^3\text{He}$  droplets doped with some inert atoms and molecular impurities have been addressed within the Finite Range Density Functional (FRDF) theory [19], that has proven to be a valuable alternative to Monte Carlo methods, which are notoriously difficult to apply to Fermi systems. Indeed, a quite accurate description of the properties of inhomogeneous liquid  $^4\text{He}$  at  $T = 0$  has been obtained within DF theory [23], and a similar approach has followed for  $^3\text{He}$  (see [19, 24] and Refs. therein).

The experiments we report have been performed in a helium droplet machine used earlier for LIF and BD studies, and is described elsewhere [2]. Briefly, helium gas is expanded under supersonic conditions from a cold nozzle forming a beam of droplets traveling freely under high vacuum conditions. The droplets are doped downstream employing the pick-up technique: in a heated scattering cell, bulk sodium is evaporated in such a way that, on average, a single metal atom is carried by each droplet. LIF absorption spectra of doped droplets are recorded upon electronic excitation using a continuous wave ring-dye laser and detection in a photo multiplier tube (PMT). Since electronic excitation of alkali-doped helium droplets is eventually followed by desorption of the chromophore, BD spectra can be registered by a Langmuir-Taylor surface ionization detector [25]. Phase-sensitive detection with respect to the chopped laser or droplet beam was used. For that reason the BD signal (cf. Fig. 2), i.e. a decrease in intensity, is directly recorded as a positive yield. For these experiments, a

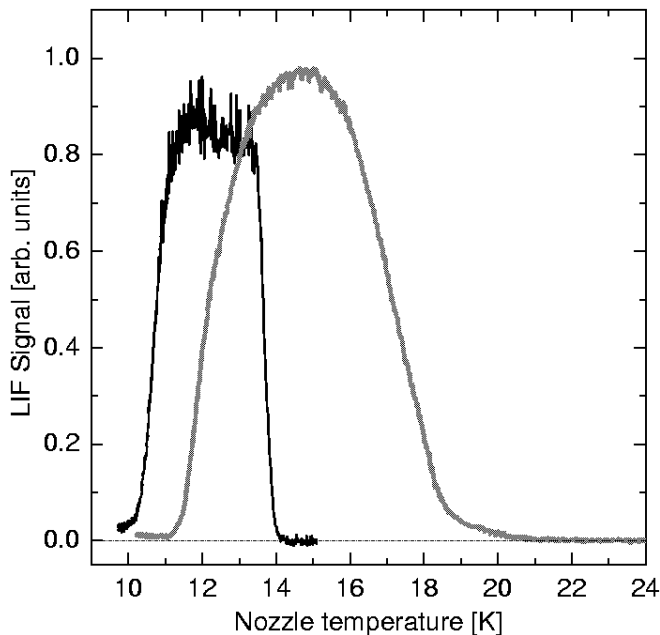


FIG. 1: Laser-induced fluorescence signal as a function of nozzle temperature forming  $^3\text{He}$  droplets (black) in comparison to  $^4\text{He}$  droplets (grey). In both runs a stagnation pressure of 20 bar was used; nozzle diameter was  $5\,\mu\text{m}$ . Normalization is such that the plot gives the correct relative intensities.

new droplet source was built to provide the necessary lower nozzle temperatures to condense  $^3\text{He}$  droplets. Expanding  $P_0 = 20$  bar of helium gas through a nozzle  $5\,\mu\text{m}$  in diameter, we now can establish temperatures down to 7.5 K using a two-stage closed cycle refrigerator (Sumitomo Heavy Industries, Model: RDK-408D). In this way, without needing any liquid helium or nitrogen for pre-cooling or cold shields, stable beam conditions can be utilized over several days.

Fig. 1 compares the number of Na-doped  $^3\text{He}$  vs.  $^4\text{He}$  droplets expanding 20 bar helium as a function of the nozzle temperature  $T_0$ . The absolute number densities in the maxima of both distributions are quite similar. The formation of droplets from a supersonic expansion is well known and thoroughly discussed in the literature: Besides the determination of absolute cluster sizes [11, 26], the size dependence as a function of source conditions has already been studied [4, 27]. The low temperature cutoff appears at source conditions where the isentrope of the expansion hits the helium critical point [28]; the disappearance at high temperatures just means that the droplets are getting too small to carry the dopant. Here, the critical size is determined by the thermal energy during pick-up which leads to evaporation of helium atoms and a destruction of small droplets. For the spectroscopic measurements presented in the following, we set  $T_0 = 11$  K for  $^3\text{He}$ , and  $T_0 = 15$  K for  $^4\text{He}$ . These conditions are expected to result in comparable mean cluster sizes around 5000 atoms per droplet [11, 26]. As far as our results are concerned, Fig. 1 demonstrates that we

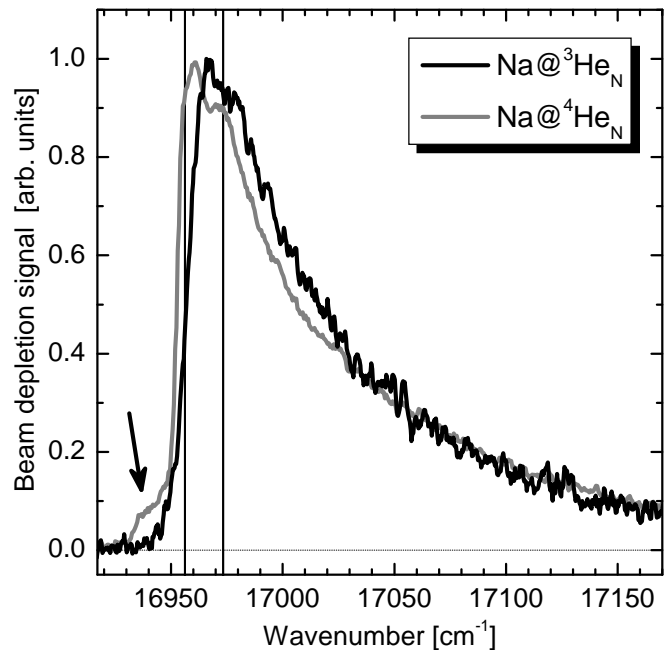


FIG. 2: Beam depletion spectra of Na atoms attached to  $^3\text{He}/^4\text{He}$  nanodroplets. The vertical lines indicate the positions of the two components of the Na gas-phase  $3p \leftarrow 3s$  transition.

see the correct formation as well as droplet sizes of the different isotopes and that we use suitable source conditions to guarantee comparable sizes.

In Fig. 2 the absorption spectrum of Na atoms attached to  $^3\text{He}$  nanodroplets is shown in comparison to Na-doped  $^4\text{He}$  droplets. We present here the BD spectra because they do not contain the strong fluorescence background lines of free Na atoms which cover the crucial steep increase of the droplet spectrum. Moreover, LIF does not always represent the total absorption spectrum because it relies on the emission of a photon in the spectral range of the PMT. Hence, absorption processes followed by either radiationless decay or emission of photons in the infrared spectral region are suppressed. The latter has been observed in LIF spectra where alkali-helium exciplexes form upon excitation of alkali atoms on the surface of  $^4\text{He}$  droplets [5, 29]. In our experiment  $\text{Na}^3\text{He}$  exciplexes are formed in the same way as their  $\text{Na}^4\text{He}$  counterparts. This became immediately obvious because we were able to discriminate the corresponding red-shifted emission intensities. However, as far as the measured absorption spectra of  $\text{Na}@^3\text{He}_N$  are concerned, the LIF data are very well in accord with the BD absorption.

The outcome of the spectrum of Na attached to  $^3\text{He}$  nanodroplets is very similar to the spectrum on  $^4\text{He}$  droplets. The asymmetrically broadened line is almost unshifted with respect to the gas-phase absorption. This absence of a shift immediately confirms the surface location because atoms embedded in bulk superfluid helium are known to evolve large blue-shifts of the order of a couple of hundreds of wavenumbers and much more

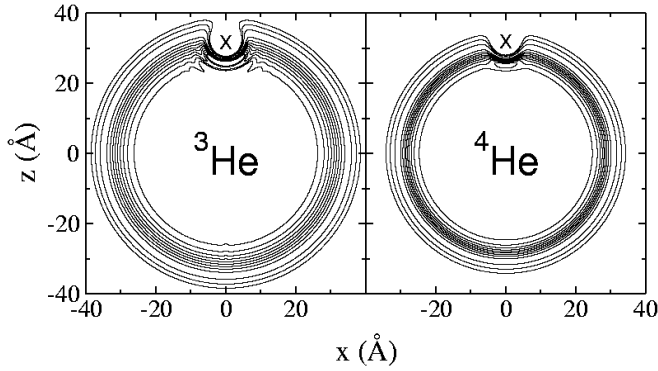


FIG. 3: Equidensity lines in the  $x-z$  plane showing the stable state of a Na atom (cross) on a  $\text{He}_{2000}$  droplet. The 9 inner lines correspond to densities  $0.9\rho_0$  to  $0.1\rho_0$ , and the 3 outer lines to  $10^{-2}\rho_0$ ,  $10^{-3}\rho_0$ , and  $10^{-4}\rho_0$  ( $\rho_0 = 0.0163 \text{ \AA}^{-3}$  for  $^3\text{He}$ , and  $0.0218 \text{ \AA}^{-3}$  for  $^4\text{He}$ ).

broadened absorption lines [30]. A blue shift is a consequence of the repulsion of the helium environment against the spatially enlarged electronic distribution of the excited state (“bubble effect”). The interaction towards the  $^3\text{He}$  droplets appears to be slightly enhanced, evidenced by the small extra blue shift of the spectrum compared to the  $^4\text{He}$  spectrum. In a simple picture this means that more helium atoms are contributing or, in other words, a more prominent “dimple” interacts with the chromophore. The upper halves of the spectra are almost identical, when shifting the  $^3\text{He}$  spectrum by  $7.5 \pm 1 \text{ cm}^{-1}$  to lower frequencies. The influence of different droplet sizes does not affect this observation: A dependence of the  $^4\text{He}$  spectra varying the droplet size is already shown in [3]. Probing smaller droplets narrows the spectrum but does not shift the observed doublet structure. The shift of the  $^3\text{He}$  spectrum would be even more conspicuous when comparing smaller droplets. Unfortunately, the corresponding small  $^3\text{He}$  droplet sizes are experimentally not accessible because within the plateau region of the droplet yield shown in Fig. 1 the droplet sizes are almost unchanged [11]. The increase in width (FWHM) of the  $^3\text{He}$  spectrum is only 7%. Taking into account the just mentioned droplet size dependence of the width, this difference might not even be significant. Regarding the substructure of the line, the only notable exception is the absence of the red-shifted shoulder, which is observed in the case of  $^4\text{He}$  and marked with an arrow in Fig. 2. This feature, which is even more pronounced in the absorption of Li-doped  $^4\text{He}$  droplets [3] has not been interpreted yet. The shift with respect to the maximum of the absorption line is  $\approx 20 \text{ cm}^{-1}$ , too high in energy to be attributed to an excited compressional or surface mode of the droplet at 0.38 K [19, 31].

FRDF calculations at  $T = 0$  confirm the picture emerging from the measurements, i.e. the surface location of Na on  $^3\text{He}$  nanodroplets causing a more pronounced “dimple” than in  $^4\text{He}$  droplets. We have investigated the stable configurations of a sodium atom on both  $^3\text{He}$  and

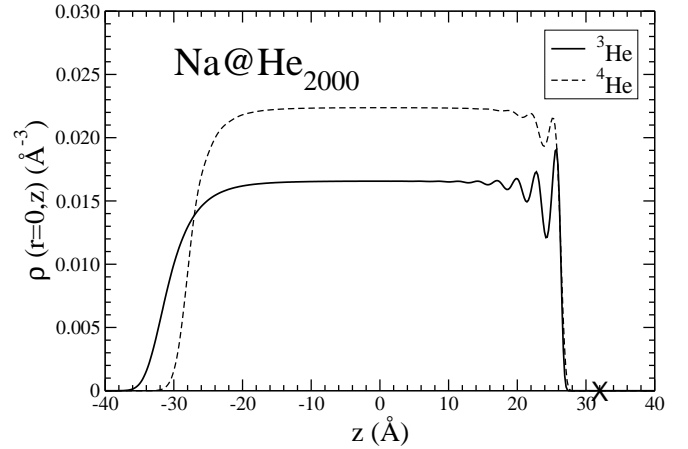


FIG. 4: Density profiles along a line connecting the impurity to the center of the cluster showing the equilibrium configuration of a Na atom (cross) on  $\text{He}_{2000}$  nanodroplets.

$^4\text{He}$  clusters of different sizes. The FRDF’s used for  $^3\text{He}$  and  $^4\text{He}$  are described in [32, 33]. The large number of  $^3\text{He}$  atoms we are considering allows to use the extended Thomas-Fermi approximation [16]. The minimization of the energy DF’s with respect to density variations, subject to the constraint of a given number of He atoms  $N$ , leads to Euler-Lagrange equations whose solution give the equilibrium particle densities  $\rho(\mathbf{r})$ . These equations have been solved as indicated in [34]. The presence of the foreign impurity is modeled by a suitable potential obtained by folding the helium density with a Na-He pair potential. We have used the potential proposed by Patil [35] to describe the impurity-He interactions. Potential energy curves describing the He-alkali interaction have been calculated recently by ab-initio methods [8], and found to agree very well with the Patil potential.

Fig. 3 shows the equilibrium configuration for a Na atom adsorbed onto  $\text{He}_{2000}$  clusters. For a given  $N$ , the size of the  $^3\text{He}_N$  droplet is larger than that of the  $^4\text{He}_N$  droplet -an obvious consequence of the smaller  $^3\text{He}$  saturation density-. Comparison with the stable state on the  $^4\text{He}_{2000}$  cluster shows that, in agreement with the experimental findings presented before, the “dimple” structure is more pronounced in the case of  $^3\text{He}$ , and that the Na impurity lies *inside* the surface region for  $^3\text{He}$  and *outside* the surface region for  $^4\text{He}$  (we recall that the surface region is usually defined as that comprised between the radii at which  $\rho = 0.1\rho_0$  and  $\rho = 0.9\rho_0$ , where  $\rho_0$  is the He saturation density [10, 11, 16]). We attribute this to the lower surface tension of  $^3\text{He}$  ( $0.113 \text{ K/\AA}^2$ ) as compared to that of  $^4\text{He}$  ( $0.274 \text{ K/\AA}^2$ ), which also makes the surface thickness of bulk liquid and droplets larger for  $^3\text{He}$  than for  $^4\text{He}$  [10, 11]. The Na-droplet equilibrium distance, here defined as the ‘radial’ distance between the impurity and the point where the density of the *pure* drop would be  $\rho \sim \rho_0/2$ , is  $R \sim 1.1 \text{ \AA}$  for  $^3\text{He}$ , and  $R \sim 3.6 \text{ \AA}$  for  $^4\text{He}$ . For the larger droplets we have studied,  $R$  is nearly  $N$ -independent. A related quantity is the defor-

mation of the surface upon Na adsorption, which can be characterized [7] by the “dimple” depth,  $\xi$ , defined as the difference between the position of the dividing surface at  $\rho \sim \rho_0/2$ , with and without impurity, respectively. We find  $\xi \sim 4.5$  Å for  $^3\text{He}$ , and  $\xi \sim 2.1$  Å for  $^4\text{He}$ . Fig. 4 shows the density profiles for  $\text{Na}@^4\text{He}_{2000}$ . Note the more diffuse liquid-vacuum interface for the  $^3\text{He}$  droplet far from the impurity, and the occurrence of more marked density oscillations (with respect to the  $^4\text{He}$  case) where the softer  $^3\text{He}$  surface is compressed by the adsorbed Na atom. Our calculations thus yield the detailed structure of the liquid around the impurity, which is an essential ingredient for any line-shift calculation of the main electronic transitions in the adatom [3] and for the understanding of dynamical processes which already have been observed in time-dependent experiments [36].

We have obtained the shift between the  $^3\text{He}$  and  $^4\text{He}$  spectra in Fig. 2 within the Frank-Condon approximation, i.e. assuming that the “dimple” shape does not change during the Na excitation. The shift is calculated within the model given in [37], evaluating Eqs. 5 and 6 therein, both for  $^3\text{He}$  and  $^4\text{He}$ . We used the excited state A  $^2\Pi$  and B  $^2\Sigma$  potentials of [8] because their Na-He GS potential is very similar to the Patil potential we have used to obtain the equilibrium configurations. For our largest droplet ( $N = 2000$ ) we find that the  $^3\text{He}$  spectrum is blue-shifted with respect to the  $^4\text{He}$  one by  $6.4\text{ cm}^{-1}$ , in good agreement with the experimental value of  $7.5 \pm 1\text{ cm}^{-1}$  as extracted from Fig. 2.

Solvation energies  $S_{Na} = E(\text{Na}@^N\text{He}) - E(^N\text{He})$  are shown in Fig. 5 as a function of droplet sizes. More negative values of  $S_{Na}$  indicate increased binding of the Na atom to the droplet surface. The lines are a fit of the form

$$S_{Na}(N) = S_0 + \frac{S_1}{N^{1/3}} + \frac{S_2}{N^{2/3}} \quad (1)$$

with  $S_0 = -12.1(-12.5)$ ,  $S_1 = -28.3(-31.6)$ , and  $S_2 = 37.3(37.6)$  K for  $^4\text{He}(^3\text{He})$ . To compare with “exact” PIMC result [8], we have calculated  $\text{Na}@^4\text{He}_{300}$ . Part of the small difference between the two values has to be attributed to our neglecting of the Na zero-point energy. The value  $S_{Na} \sim -12$  K has been obtained within FRDF

theory for Na adsorbed on the *planar* surface of  $^4\text{He}$  [7], which corresponds to the  $N = \infty$  limit in this figure.

Our results show that Na adsorption on  $^3\text{He}$  droplets occurs in very much the same way as in the case of  $^4\text{He}$ , i.e., the adatom is located on the surface, though in a slightly more pronounced “dimple”. The similarities in the experimental spectra are certainly remarkable for two apparently very different fluids, one normal and the other superfluid, and clearly indicate that superfluidity does not play any substantial role in the processes described here. This is likely a consequence of the very fast time scale characterizing the Na electronic excita-

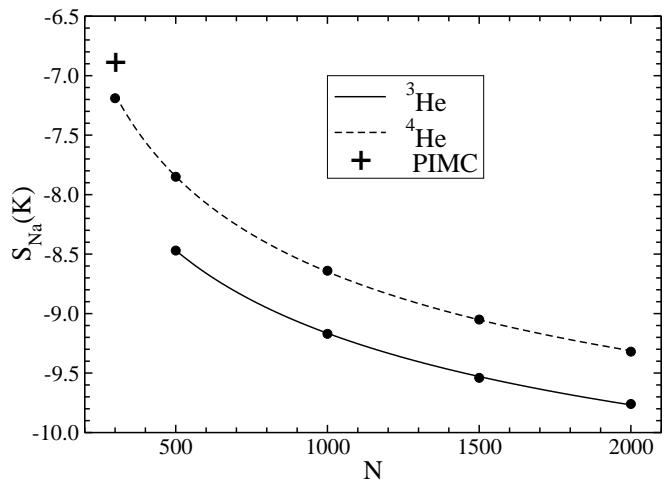


FIG. 5: Na solvation energy as a function of  $N$ . The cross is the PIMC result of [8].

is due to the different structure of the “dimple”, which accounts for the small shift in their spectra observed in the experiments and found in our calculations as well.

We thank Flavio Toigo for useful comments. This work has been supported by grants MIUR-COFIN 2001 (Italy), BFM2002-01868 from DGI (Spain), and 2001SGR-00064 from Generalitat of Catalunya as well as the DFG (Germany).

[1] F. Stienkemeier and A. F. Vilesov, J. Chem. Phys. **115**, 10119 (2001).  
[2] F. Stienkemeier, F. Meier, and H. O. Lutz, J. Chem. Phys. **107**, 10816 (1997); Eur. Phys. J. D **9**, 313 (1999).  
[3] F. Stienkemeier, J. Higgins, C. Callegari, S. I. Kanorsky, W. E. Ernst, and G. Scoles, Z. Phys. D: At., Mol. Clusters **38**, 253 (1996).  
[4] F. Stienkemeier, W. E. Ernst, J. Higgins, and G. Scoles, J. Chem. Phys. **102**, 615 (1995);  
[5] C. Callegari, J. Higgins, F. Stienkemeier, and G. Scoles, J. Phys. Chem. A **102**, 95 (1998).  
[6] F. Brühl, R. Trasca, and W. E. Ernst, J. Chem. Phys.

**115**, 10220 (2001).  
[7] F. Ancilotto, E. Cheng, M. W. Cole, and F. Toigo, Z. Phys. B: Condens. Matter **98**, 323 (1995).  
[8] A. Nakayama and K. Yamashita, J. Chem. Phys. **114**, 780 (2001).  
[9] J. Reho, C. Callegari, J. Higgins, W. E. Ernst, K. K. Lehmann, and G. Scoles, Faraday Discuss. **108**, 161 (1997).  
[10] F. Dalfovo, J. Harms, and J. P. Toennies, Phys. Rev. B **58**, 3341 (1998).  
[11] J. Harms, P. J. Toennies, M. Barranco, and M. Pi, Phys. Rev. B **63**, 184513 (2001).

- [12] J. P. Toennies and A. F. Vilesov, *Annu. Rev. Phys. Chem.* **49**, 1 (1998); K. K. Lehmann and G. Scoles, *Science* **279**, 2065 (1998), J. P. Toennies, A. F. Vilesov, and K. B. Whaley, *Physics Today* **54**, 31 (2001).
- [13] C. Callegari, A. Conjusteau, I. Reinhard, K. K. Lehmann, G. Scoles, and F. Dalfovo, *Phys. Rev. Lett.* **83**, 5058 (1999); **84**, 1848(E) (2000); Y. Kwon, P. Huang, M. V. Patel, D. Blume, and K. B. Whaley, *J. Chem. Phys.* **113**, 6469 (2000); E. W. Draeger and D. M. Ceperley, *Phys. Rev. Lett.* **90**, 65301 (2003); R. Brühl, R. Guardiola, A. Kalinin, O. Kornilov, J. Navarro, T. Savas, and J. P. Toennies, *ibid.* **92**, 185301 (2004).
- [14] J. Harms, M. Hartmann, J. P. Toennies, A. F. Vilesov, and B. Sartakov, *J. Mol. Spectrosc.* **185**, 204 (1997).
- [15] V. R. Pandharipande, S. C. Pieper, and R. B. Wiringa, *Phys. Rev. B* **34**, 4571 (1986).
- [16] S. Stringari and J. Treiner, *J. Chem. Phys.* **87**, 5021 (1987).
- [17] M. Barranco, J. Navarro, and A. Poves, *Phys. Rev. Lett.* **78**, 4729 (1997).
- [18] Ll. Serra, J. Navarro, M. Barranco, and Nguyen Van Giai, *Phys. Rev. Lett.* **67**, 2311 (1991); S. Weisgerber and P.-G. Reinhard, *Z. Phys. D: At., Mol. Clusters* **23**, 275 (1992); M. Barranco, D. M. Jezek, E. S. Hernández, J. Navarro, and Ll. Serra, *ibid.* **28**, 257 (1993).
- [19] F. Garcias, Ll. Serra, M. Casas, and M. Barranco, *J. Chem. Phys.* **108**, 9102 (1998); *ibid.* **115**, 10154 (2001).
- [20] R. Guardiola, *Phys. Rev. B* **62**, 3416 (2000).
- [21] S. Grebenev, J. P. Toennies, and A. F. Vilesov, *Science* **279**, 2083 (1998).
- [22] A. Griffin and S. Stringari, *Phys. Rev. Lett.* **76**, 259 (1996); E. W. Draeger and D. M. Ceperley, *ibid.* **89**, 015301 (2002).
- [23] F. Dalfovo, A. Lastri, L. Pricapenko, S. Stringari, and J. Treiner, *Phys. Rev. B* **52**, 1193 (1995).
- [24] E. S. Hernández and J. Navarro, in *Microscopic Approaches to Quantum Liquids in Confined Geometries*, E. Krotscheck and J. Navarro Eds. pag. 261 (World Sci., Singapore, 2002).
- [25] F. Stienkemeier, M. Wewer, F. Meier, and H. O. Lutz, *Rev. Sci. Instr.* **71**, 3480 (2000).
- [26] J. Harms and J. P. Toennies, unpublished results.
- [27] A. Scheidemann, J. P. Toennies, and J. A. Northby, *Phys. Rev. Lett.* **64**, 1889 (1990).
- [28] J. Harms, J. P. Toennies, and E. Knuth, *J. Chem. Phys.* **106**, 3348 (1997).
- [29] J. Reho, J. Higgins, C. Callegari, K. K. Lehmann, and G. Scoles, *J. Chem. Phys.* **113**, 9686 (2000).
- [30] Y. Takahashi, K. Sano, T. Kinoshita, and T. Yabuzaki, *Phys. Rev. Lett.* **71**, 1035 (1993).
- [31] M. Casas and S. Stringari, *J. Low Temp. Phys.* **79**, 135 (1990); S. A. Chin and E. Krotscheck, *Phys. Rev. B* **45**, 852 (1992); *ibid.* **52**, 10405 (1995). M. Barranco and E. S. Hernández, *ibid.* **49**, 12078 (1994).
- [32] M. Barranco, M. Pi, E. S. Hernández, and J. Navarro, *Phys. Rev. B* **56**, 8997 (1997).
- [33] R. Mayol, M. Pi, M. Barranco, and F. Dalfovo, *Phys. Rev. Lett.* **87**, 145301 (2001).
- [34] M. Barranco, M. Guilleumas, E. S. Hernández, R. Mayol, M. Pi, and L. Szybisz, *Phys. Rev. B* **68**, 024515 (2003).
- [35] S. H. Patil, *J. Chem. Phys.* **94**, 8089 (1991).
- [36] O. Bünermann et al., unpublished (2004).
- [37] S. I. Kanorsky, M. Arndt, R. Dziewior, A. Weis, and T. W. Hänsch *Phys. Rev. B* **50**, 6296 (1994).